



Mid-Infrared Spectroscopic Properties of Infrared Ultra- Luminous QSOs (IR QSOs)

Chen CAO, Xiaoyang XIA,
Hong WU, Zugan DENG, &
Caina HAO

30 Aug. 2007, Torun, Poland

Background

IR QSOs

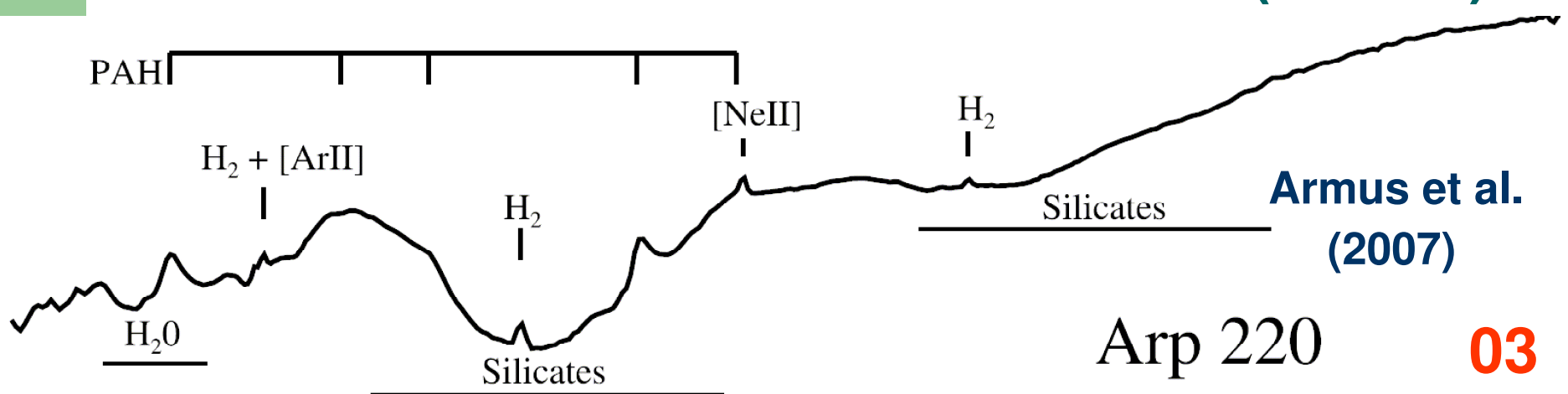
- **Infrared Ultra-Luminous QSOs :**
ULIRGs ($L_{IR} > 10^{12} L_{\odot}$) + Type 1 AGN
(optical) → IR QSOs (Zheng et al. [2002];
Hao, C.N. et al. [2005])
- **Transitional Objects from ULIRGs to**
optically selected QSOs (Canalizo & Stockton
[2000, 2001]; Hao, C.N. et al. [2005])
- **Crucial to understanding the probable**
evolutionary link between ULIRGs and
QSOs (Sanders et al. [1988] etc.)

Background



-- IRS 5-40 μm Probe →

- * 6.2, 7.7, 8.6, 11.3, 12.7 μm PAHs (SFR?!)
- * mid-IR fine-structure lines (SFR/AGN)
- * 9.7, 18 μm broad Silicate features (dust)
- * warm-to-hot dust continuum emission (AGN?!)



Arp 220

03

Sample

Object (1)	Redshift (2)	$\log(L_{\text{IR}}/L_{\odot})$ (3)	$\log(L_{60\mu\text{m}}/L_{\odot})$ (4)	$\log(L_{\text{opt}}/L_{\odot})$ (5)	RFe (6)
IR QSOs					
I Zw 1(PG 0050+124)	0.511	11.970	11.310	11.050	1.47 ^a
F00275–2859	0.2781	<12.713	12.342	11.568	1.47
F0148+3254(3C 48)	0.3670	<13.018	12.648	11.991	1.49 ^b
F01572+0024(MCG +0-0-2)	0.3010	12.622	12.622	11.142	1.13
F02054+0835	0.3450	<13.121	12.466	11.819	2.42
F07398+6552	0.1488	12.058	12.141	11.783	2.75
F11119+2257	0.1890	12.663	12.322	12.089	1.12
F12225+0210(2C 272)	0.1582	12.811	12.262	12.427	0.66
F12540+3708(MCG +1-3-1)	0.2410	12.549	12.236	11.467	1.83
F13218+0552 ⁱ	0.2051	12.728	12.270	11.467	0.48 ^c
F13342+3942	0.1311	12.549	12.445	11.821	0.73
F14026+4341	0.2232	12.960	12.445	11.930	1.33 ^b
F1539+48.51(1C 1543+4891)	0.3096	12.184	12.544	11.843	0.86 ^a
F15462–0450	0.0998	<12.250	11.995	10.381	1.32
F16136+6550(PG 1613+658)	0.1290	<12.003	11.533	11.550	0.43
F17002+5113(PG 7-113)	0.1660	12.660	11.900	11.111	1.56 ^a
F18216+3115	0.0570	12.155	12.477	12.607	0.39
F20036–1547	0.1919	<12.670	12.359	11.566	2.74
F21210–1752	0.0221	11.991	11.311	11.552	1.62

* IR QSOs: Hao05 + F14026 (HyLIRG+BALQ)

→ available: 19 (15 have both low & high –res obs.)

* ULIRGs (non-S1):

from *IRAS* 1-Jy sample and *Spitzer* GTO #105

+ High-res mid-IR data from Farrah et al. (2007)

* PG QSOs: mainly from *Spitzer* GTO & GO #14,

3187 & 20142, with enough S/N, $z < 0.27$

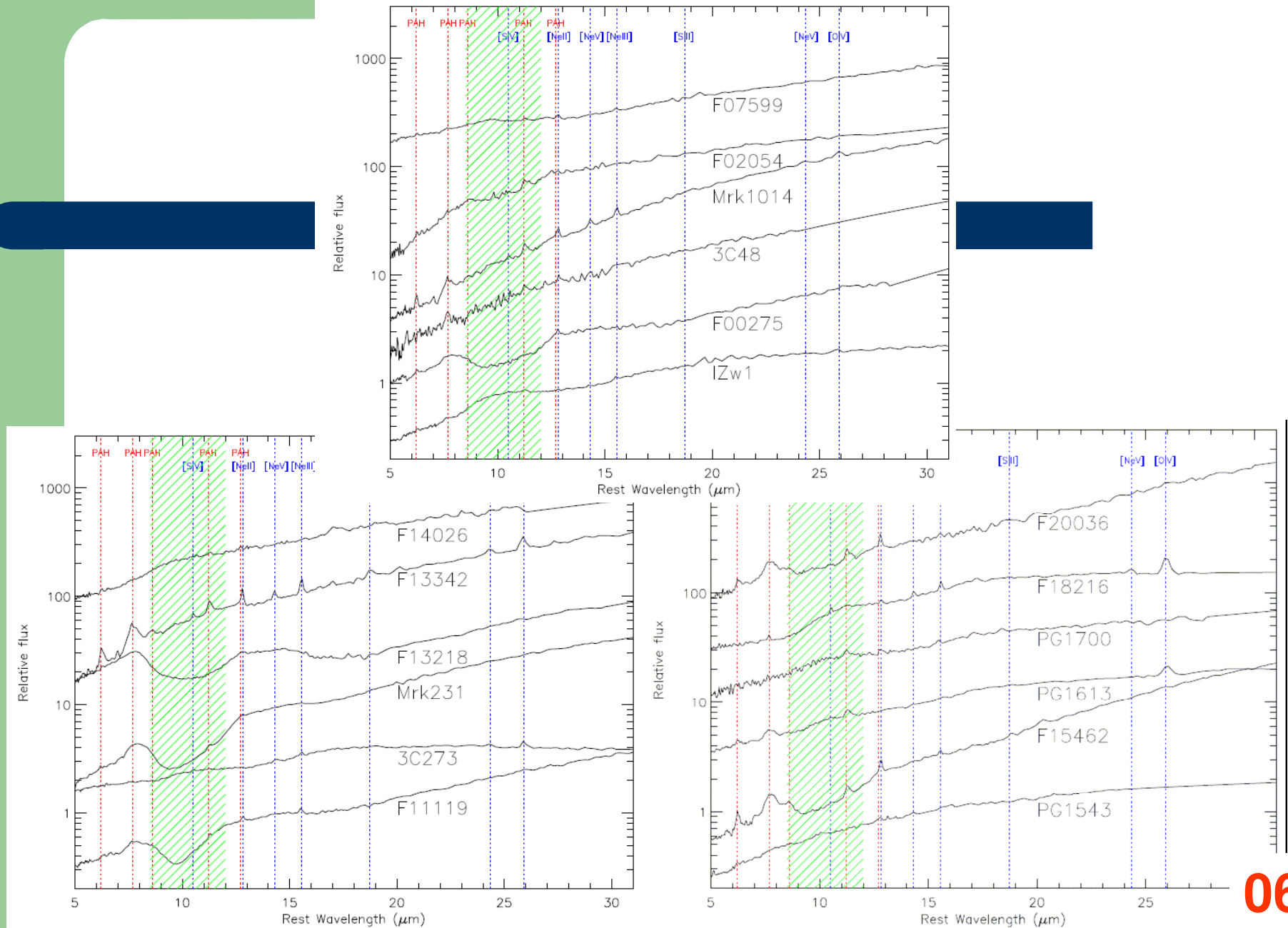
+ PG QSOs from QUEST.I (Schweitzer et al. [2006])

Data Reduction

- **Spectral Extraction:** SMART software (by IRS team of Cornell Univ.)
- **Scaling** the spectra: use 12 & 25 μ m flux densities from *IRAS* or *ISO*
- Measuring **PAH & fine-structure lines** (following Desai et al. [2007]; Farrah et al. [2007]; Schweitzer et al. [2006])
- Fitting the **continua** & measuring **silicate strengths** (following Spoon et al. [2007])

Results

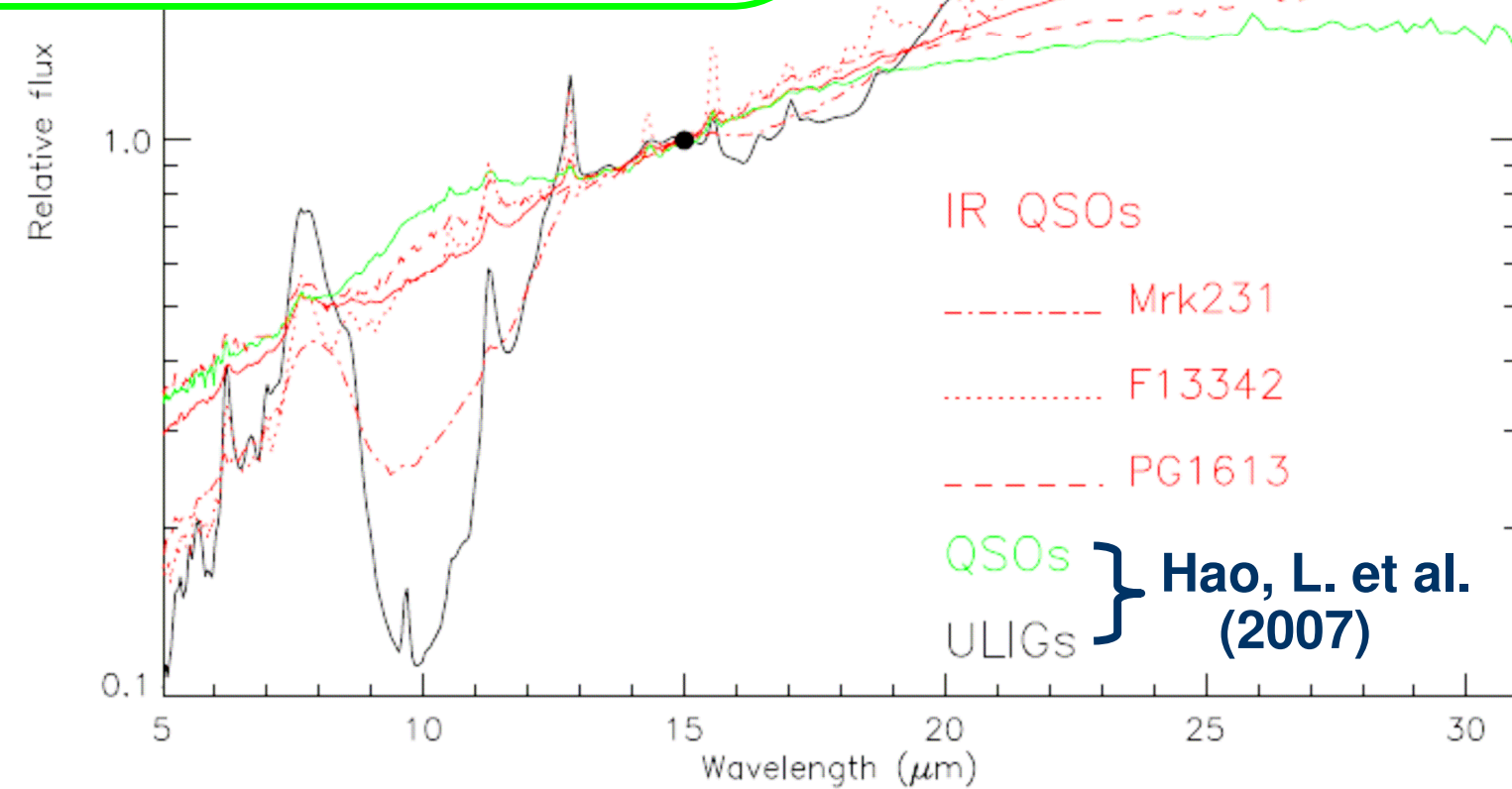
Low-Res Spectra of IR QSOs



Results

Average Spectra

The mid-IR spectral properties (continuum slope; PAH; Silicate) of **IR QSOs** are intermediate between that of **ULIRGs** & optically selected **QSOs**



Results

Histograms

IR
QSOs

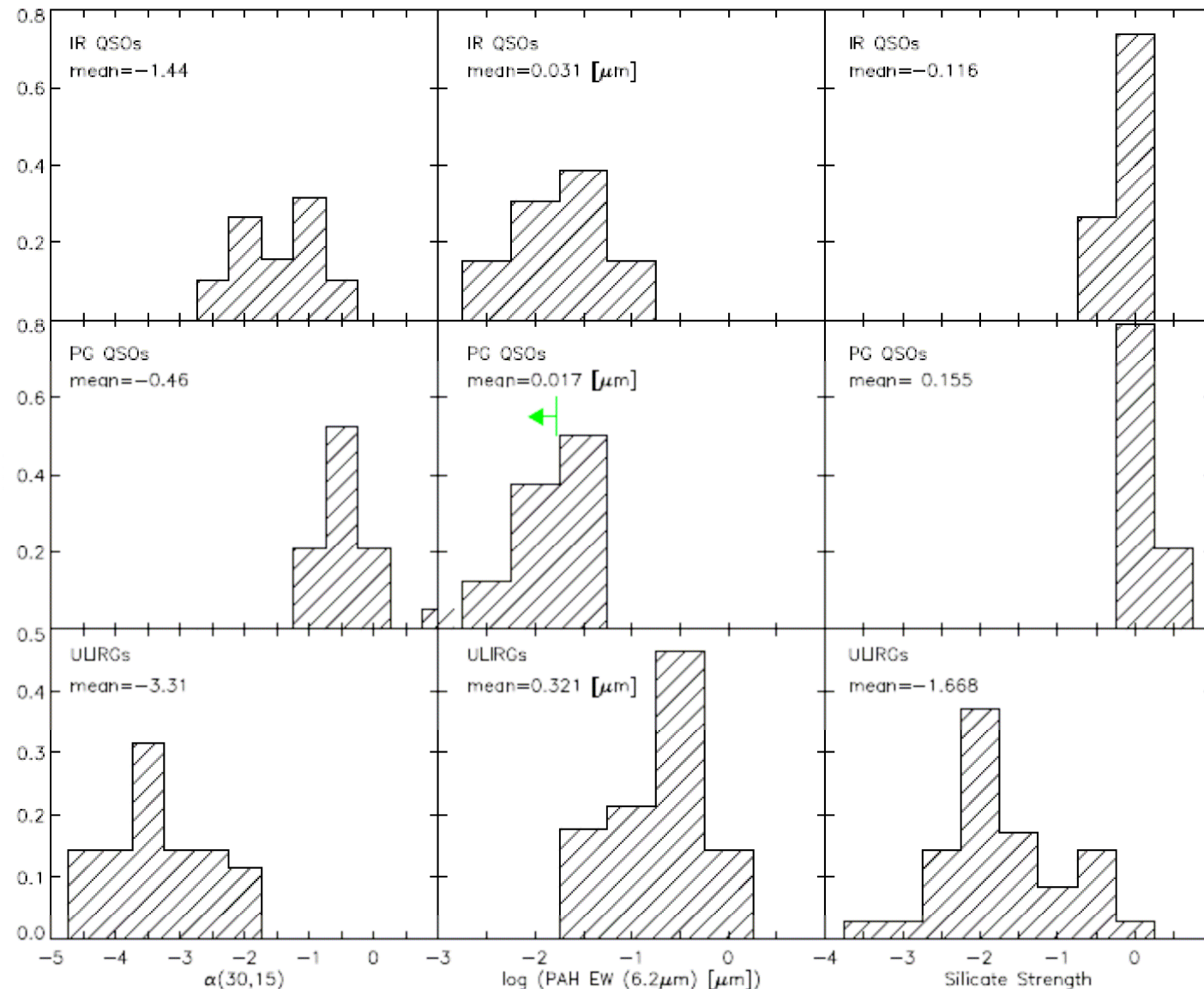
PG
QSOs

ULIRGs

$\alpha(30,15)$

EW(PAH)

S_{sil}

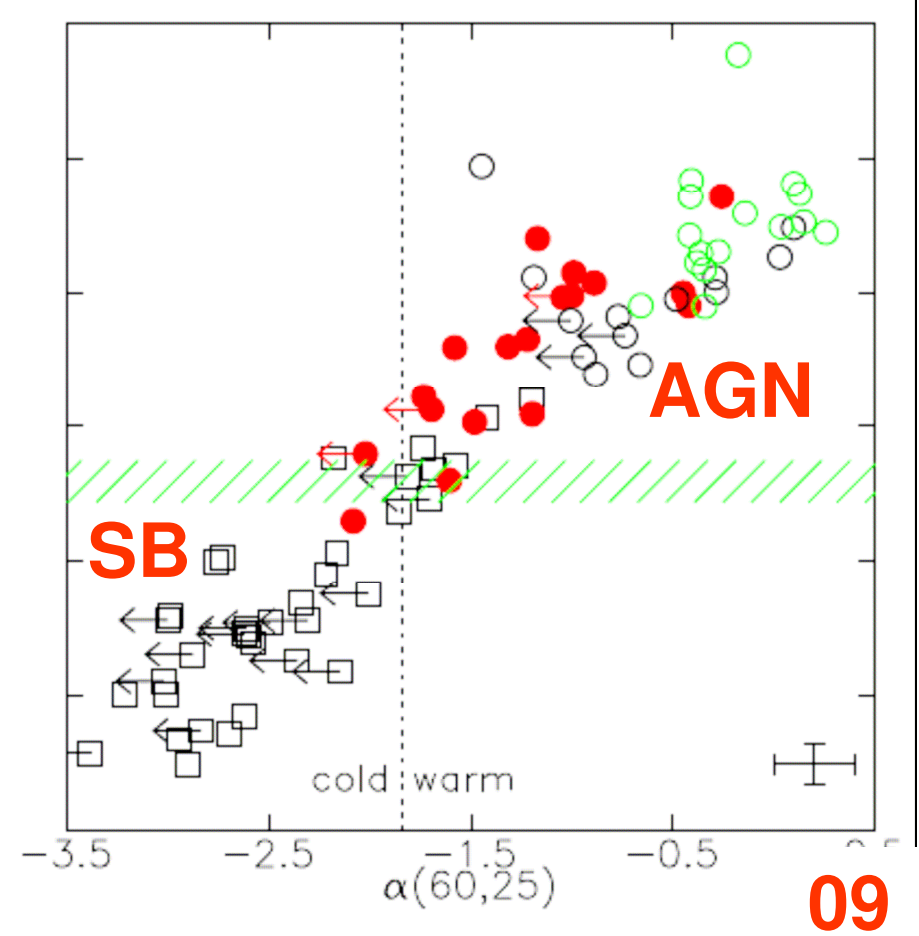
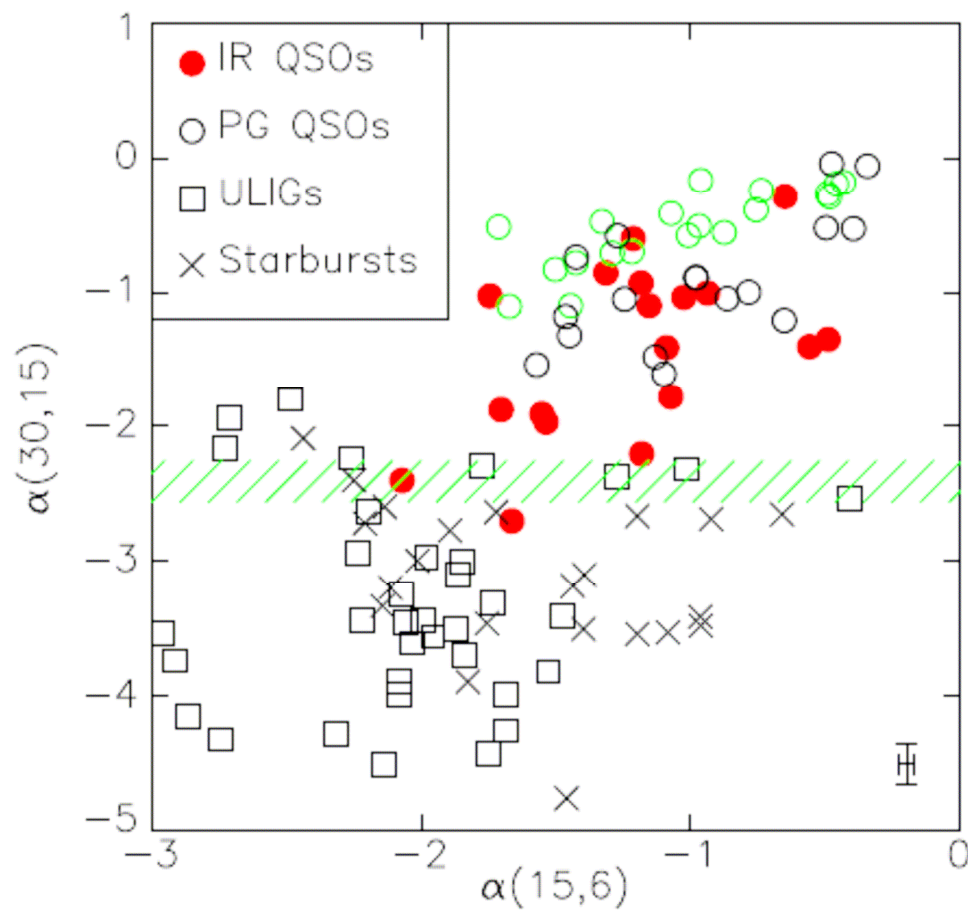


Mid-IR Diagnostics of SB and AGN activities (i)

Mid- and Far-IR color-color diagrams

$\alpha(15,6)$ vs. $\alpha(30,15)$

$\alpha(60,25)$ vs. $\alpha(30,15)$



09

Mid-IR Diagnostics of SB and AGN activities

(ii)

$\alpha(30,15)$

EW
($6.2\mu\text{m}$ PAH)

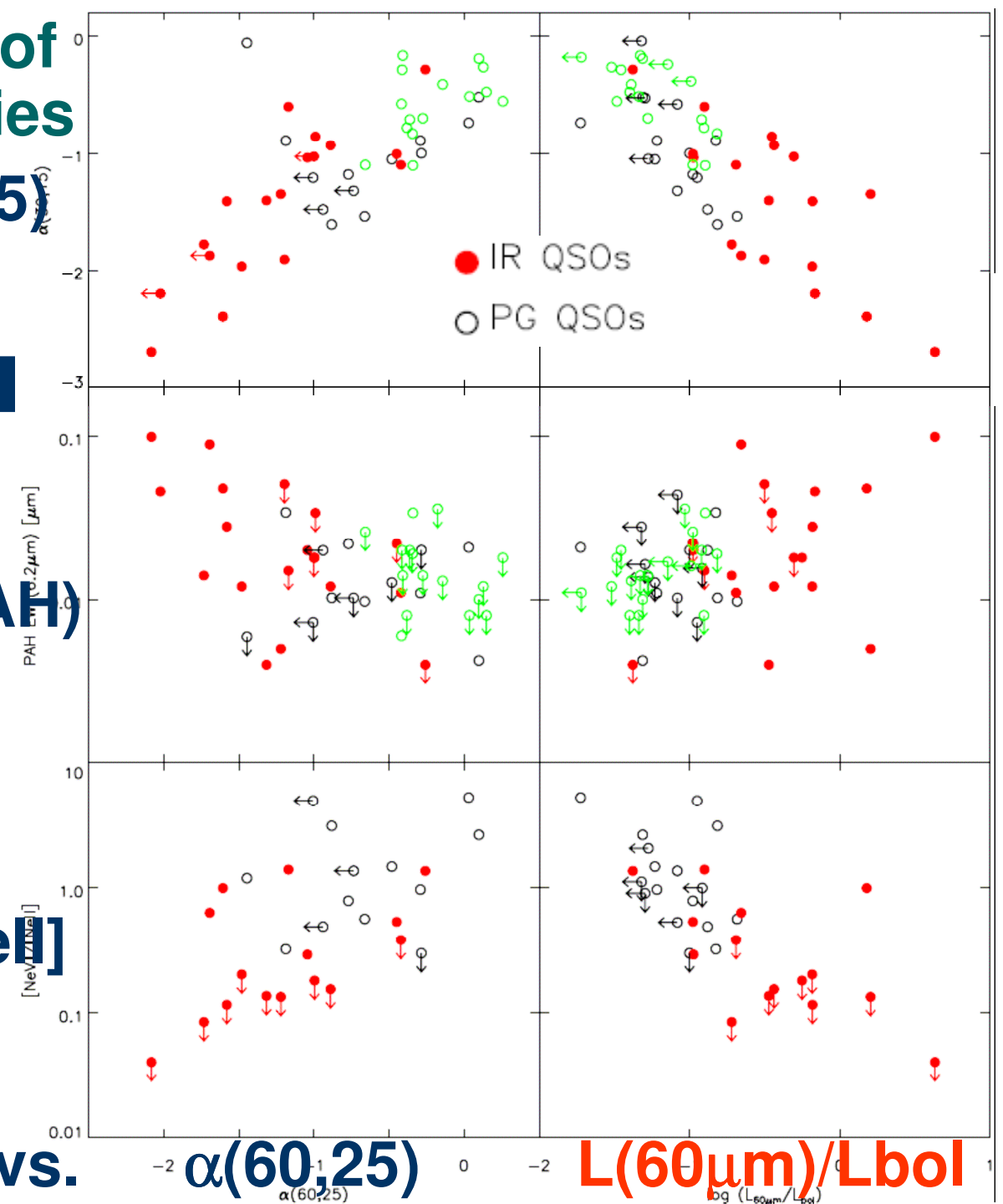
[NeV]/[NeII]

10

vs.

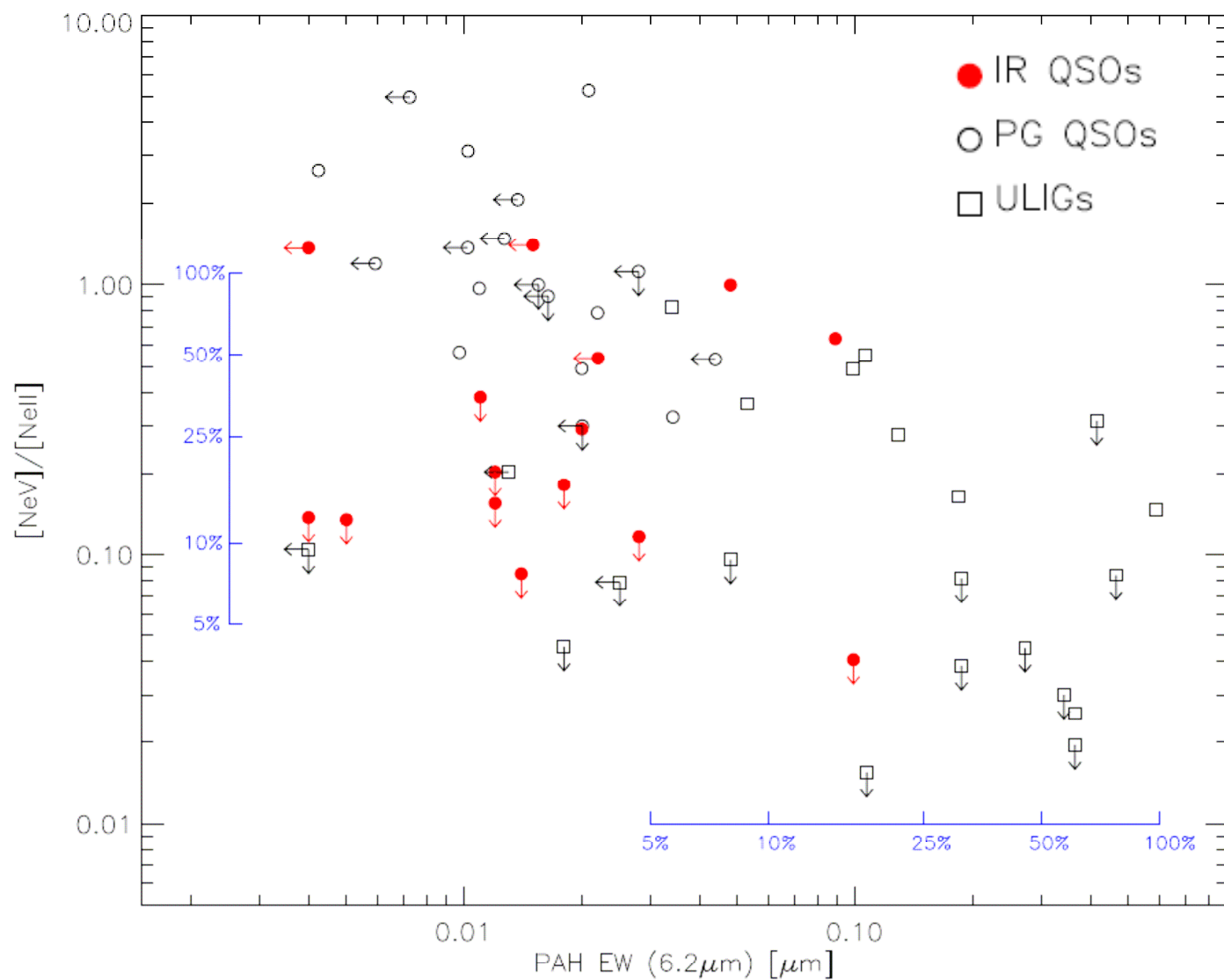
$\alpha(60,25)$

$L(60\mu\text{m})/\text{L}_{\text{bol}}$



Mid-IR Diagnostics of SB and AGN activities (iii)

Genzel Diagram -- EW(PAH) vs. [NeV]/[Nell]



Results

SFRs in QSOs & ULIRGs

-- Far-IR (60μm) : Hao, C.N. et al. (2005, 2007)

$$SFR = 3.26M_{\odot}yr^{-1} \frac{L_{60\mu m}}{10^{10}L_{\odot}}$$

$$\log(L_{60\mu m}(AGN)/L_{\odot}) = 0.794\log(\lambda L_{\lambda}(5100\text{\AA})/L_{\odot}) + 2.016$$

-- PAH emission (6.2μm): Brandl et al. (2006)

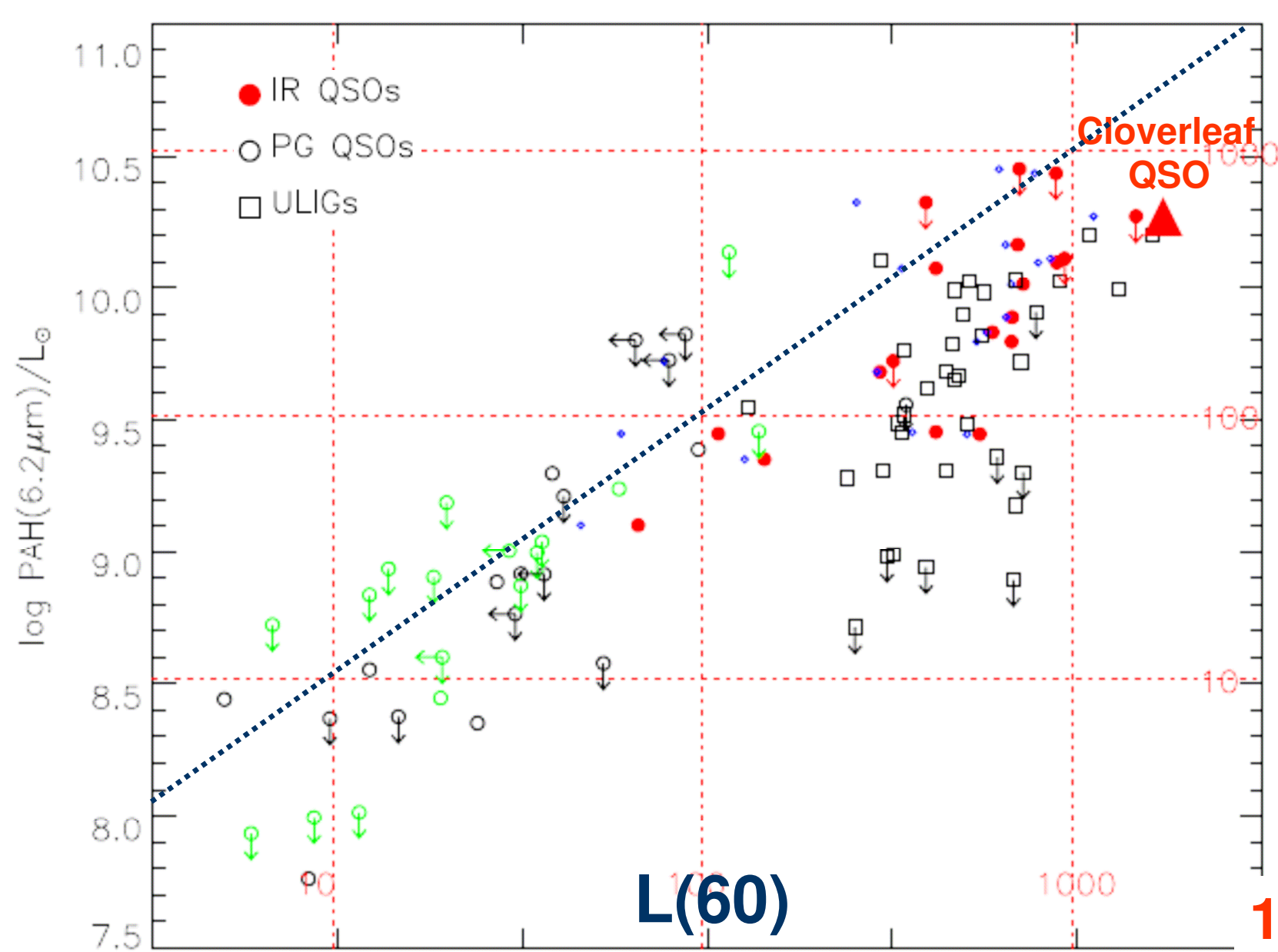
$$\log(L_{\text{IR}}^{PAH}) = 1.13 \times \log(F_{6.2\mu m\text{PAH}}D^2)$$

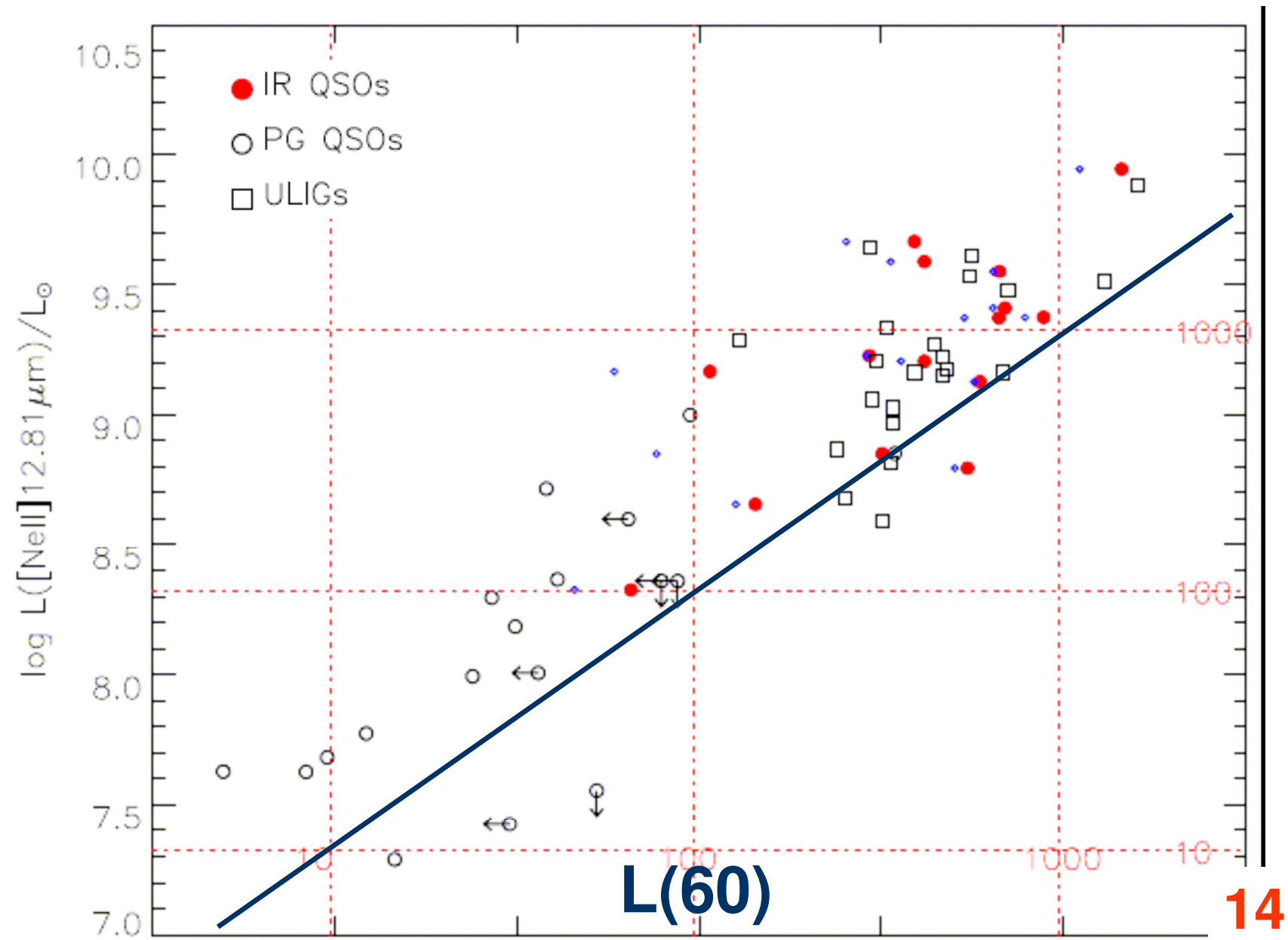
-- [NII] emission line: Ho & Keto (2006)

$$\log L_{\text{NeII}} = (1.01 \pm 0.054) \log L_{\text{IR}} - (3.44 \pm 0.56)$$

SFRs in QSOs

Comparison (i): L(60) vs. L(PAH)

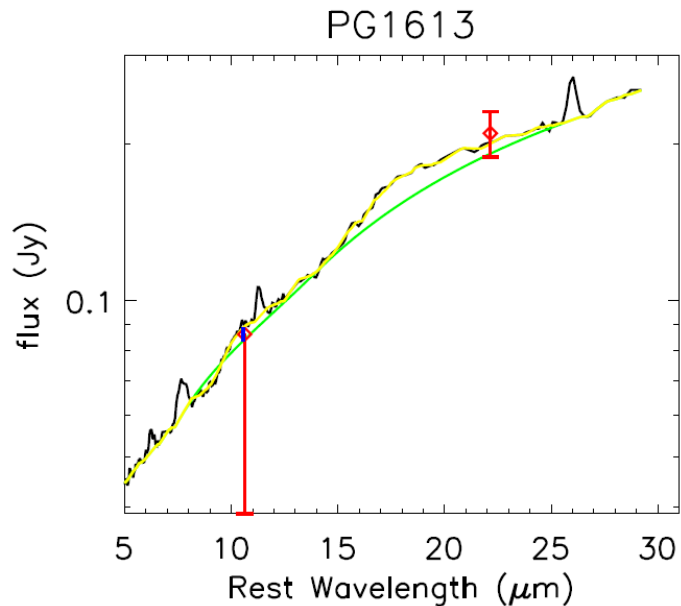




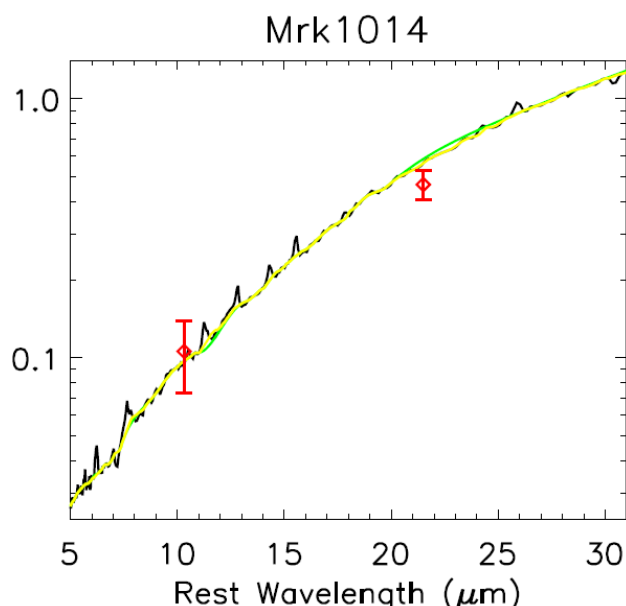
Discussion

Classification of IR QSOs

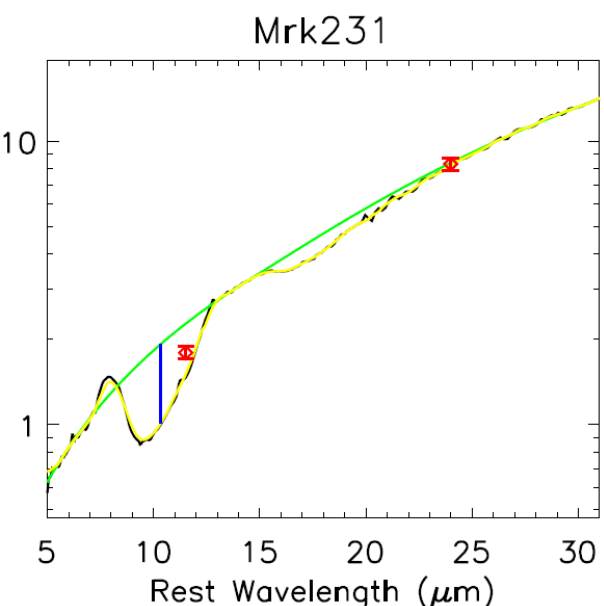
(pre)-Classical QSO



SB + QSO



ULIRG + QSO



$\langle \alpha(30,15) \rangle$ **-0.83**

-2.29

-1.72

$\langle \text{EW(PAH)} \rangle$ < 0.017

0.071

0.018

$\langle S_{\text{sil}} \rangle$ **0.08**

-0.14

-0.53

15

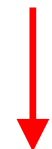
Discussion

Evolution of dust in IR QSOs

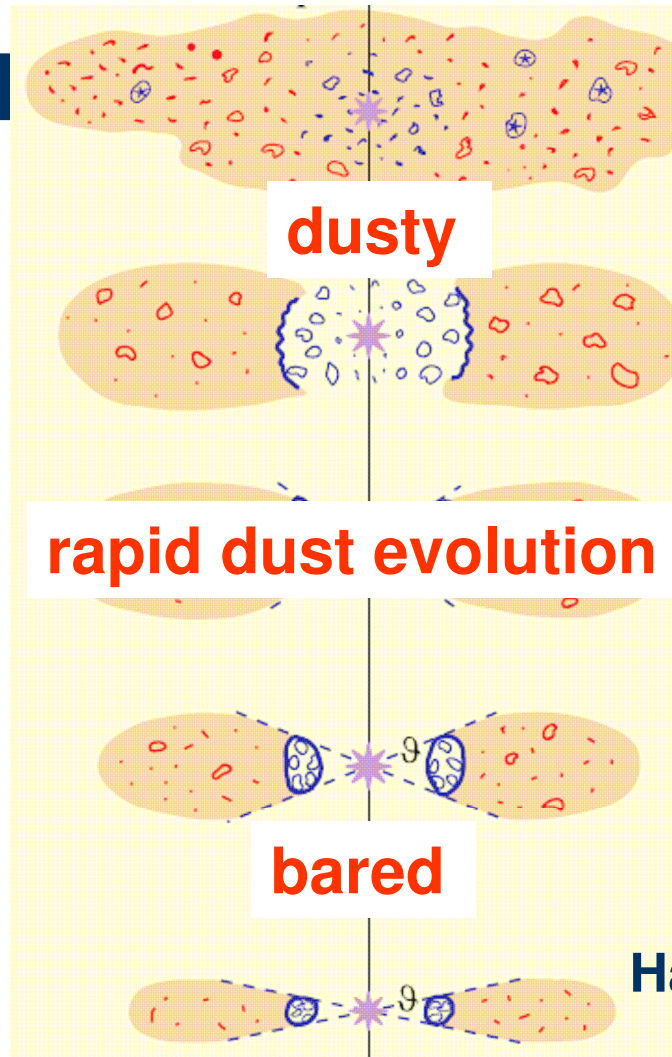
ULIRGs



IR QSOs



PG QSOs



$\langle S_{\text{sil}} \rangle$

-1.67

-0.12

+0.16

Haas et al.
(2003)

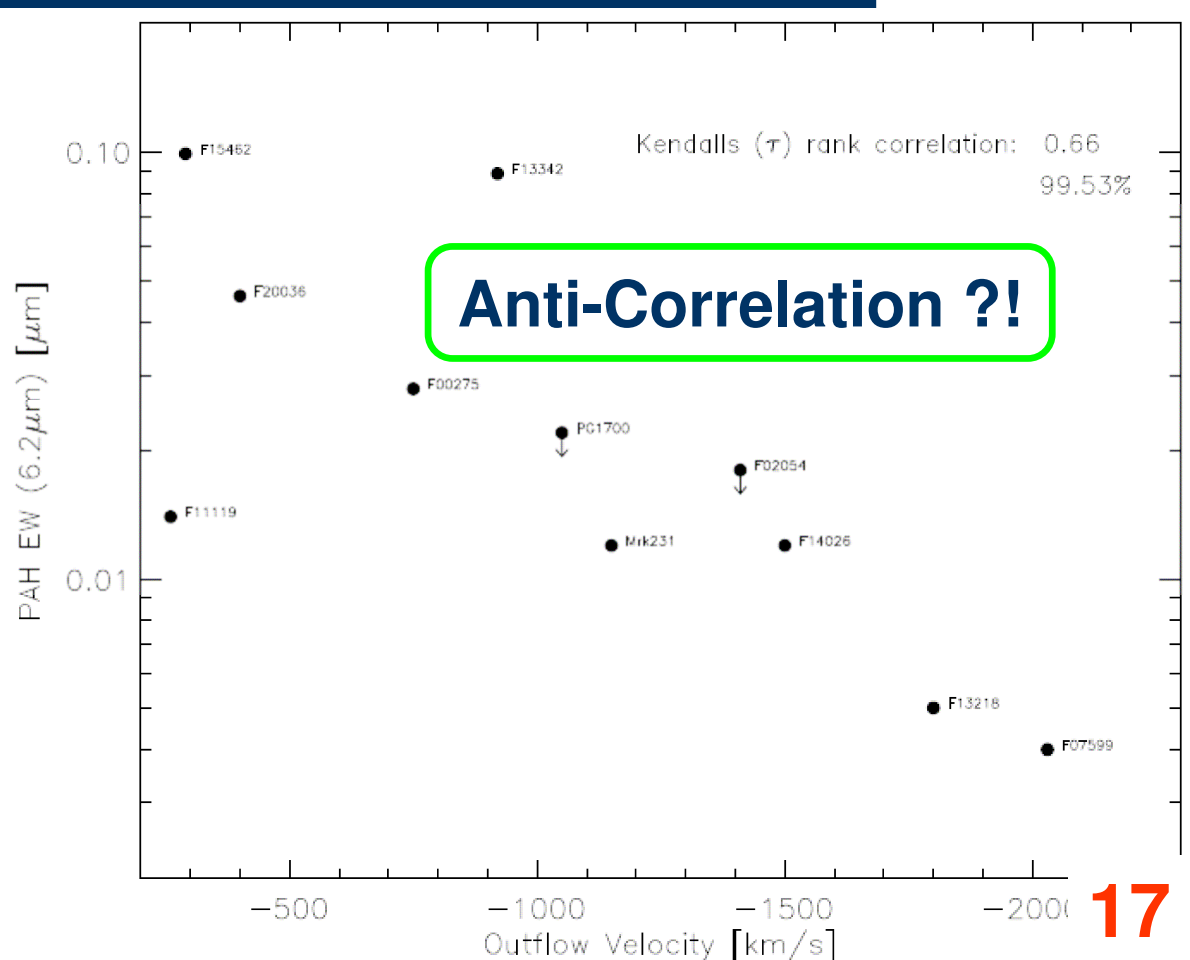
16

Discussion

Star Formation suppressed caused by AGN feedback ?!

— Outflowing Velocity : the offset broad H β emission
(Zheng et al. [2002])

— SFR/Mdot:
EW (6.2 μ m PAH)





中国科学院国家天文台

NATIONAL ASTRONOMICAL OBSERVATORIES
CHINESE ACADEMY OF SCIENCES

Chen CAO

National Astronomical Observatories,
Chinese Academy of Sciences

Datun Road A20, Chaoyang District
Beijing 100012, China

caochen@bao.ac.cn